

Combined Mutagenesis and Kinetics Characterization of the Bilin-Binding GAF Domain of the Protein Slr1393 from the Cyanobacterium *Synechocystis* PCC6803

Xiu-Ling Xu,^[a] Alexander Gutt,^[a] Jonas Mechelke,^[a] Sarah Raffelberg,^[a] Kun Tang,^[a, b] Dan Miao,^[b] Lorena Valle,^[c] Claudio D. Borsarelli,^[c] Kai-Hong Zhao,^{*,[b]} and Wolfgang Gärtner^{*,[a]}

The gene *slr1393* from *Synechocystis* sp. PCC6803 encodes a protein composed of three GAF domains, a PAS domain, and a histidine kinase domain. GAF3 is the sole domain able to bind phycocyanobilin (PCB) as chromophore and to accomplish photochemistry: switching between a red-absorbing parental and a green-absorbing photoproduct state ($\lambda_{\text{max}} = 649$ and 536 nm, respectively). Conversions in both directions were followed by time-resolved absorption spectroscopy with the separately expressed GAF3 domain of Slr1393. Global fit analysis of the recorded absorbance changes yielded three lifetimes (3.2 μs , 390 μs , and 1.5 ms) for the red-to-green conversion, and 1.2 μs , 340 μs , and 1 ms for the green-to-red conversion. In addition to the wild-type (WT) protein, 24 mutated proteins were studied spectroscopically. The design of these site-directed mutations was based on sequence alignments with related proteins and by employing the crystal structure of AnPixJg2 (PDB ID: 3W2Z), a Slr1393 orthologous from *Anabaena* sp.

PCC7120. The structure of AnPixJg2 was also used as template for model building, thus confirming the strong structural similarity between the proteins, and for identifying amino acids to target for mutagenesis. Only amino acids in close proximity to the chromophore were exchanged, as these were considered likely to have an impact on the spectral and dynamic properties. Three groups of mutants were found: some showed absorption features similar to the WT protein, a second group showed modified absorbance properties, and the third group had lost the ability to bind the chromophore. The most unexpected result was obtained for the exchange at residue 532 (N532Y). In vivo assembly yielded a red-absorbing, WT-like protein. Irradiation, however, not only converted it into the green-absorbing form, but also produced a 660 nm, further-red-shifted absorbance band. This photoproduct was fully reversible to the parental form upon green light irradiation.

Introduction


Bilin-binding photochromic proteins were for long time synonymous with "classical" phytochromes, initially identified in plants where they act as master regulators of plant photomorphogenesis.^[1] The cyanobacterial orthologues also show the phytochrome-characteristic photochromic behavior ($\lambda_{\text{max}} = 650$ and 710 nm for the red-absorbing (Pr) and far-red-absorbing (Pfr) forms, respectively), except for a blue shift (~ 10 nm)

due to the presence of phycocyanobilin (PCB) rather than the plant-specific phytylchromobilin (P Φ B) chromophore (Scheme 1). Phytochrome-like proteins employing biliverdin IX α as the chromophore (bacteriophytochromes) have also been identified, followed by the finding of chromoproteins that are generated in a red-absorbing parental state, yet in the Pfr-typical *E*-configuration of the chromophore, these undergo hypsochromic shift to the moderately stable *Z*-configuration of the chromophore (for a comprehensive overview see ref. [2]). All these chromoproteins have a three-domain architecture, PAS-GAF-(PHY),¹ that is necessary for the spectral properties.^[2, 3] All phytochrome variants studied so far (including the one investigated here, which bears a cyanobacteriochrome (CBCR) GAF domain; see next paragraph) carry the chromophore in a protonated form; whereas three pyrrolic nitrogen atoms in bilins carry a proton at neutral pH, the fourth is usually unprotonated. Incorporation into a phytochrome protein pocket

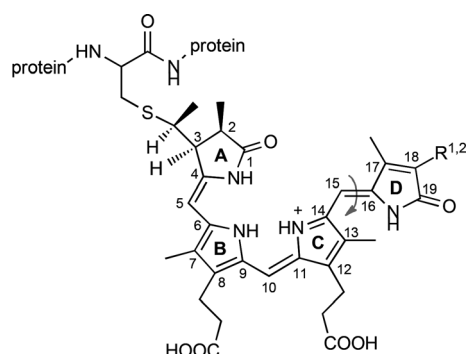
[a] Dr. X.-L. Xu, A. Gutt, J. Mechelke, Dr. S. Raffelberg, K. Tang, Prof. W. Gärtner
Max-Planck-Institute for Chemical Energy Conversion
Stiftstrasse 34-36, 45470 Mülheim (Germany)
E-mail: Wolfgang.gaertner@cec.mpg.de

[b] K. Tang, D. Miao, Prof. K.-H. Zhao
State Key Laboratory of Agricultural Microbiology
Huazhong Agricultural University
Honshanqu nanhu, Shizishan 1, Wuhan, 430070 (PR China)
E-mail: khzhao@163.com

[c] L. Valle, Prof. C. D. Borsarelli
Laboratorio de Cinética y Fotoquímica, CITSE-CONICET
Facultad de Agronomía y Agroindustrias
Universidad de Santiago del Estero (UNSE)
RN9, km 1125, 4200 Santiago del Estero (Argentina)

 Supporting information for this article is available on the WWW under <http://dx.doi.org/10.1002/cbic.201400053>.

¹ PAS: period circadian protein, Ah receptor nuclear translocator protein, and single-minded protein domain; GAF: cGMP phosphodiesterase, adenylyl cyclase and FhlA protein domain; PHY: phytochrome-characteristic protein domain.



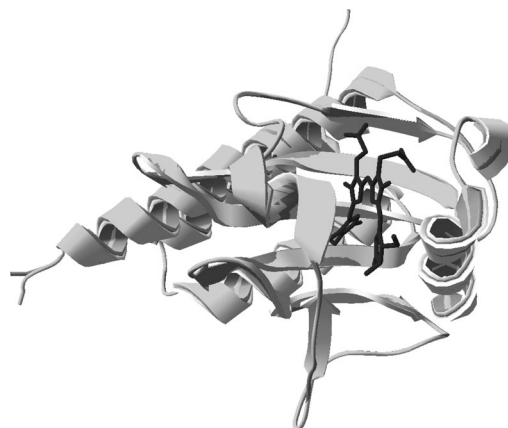
Scheme 1. Structural formulae of chromophores of canonical phytochromes and of (R²) CBCR GAF proteins in the protein-bound state. R¹=vinyl (phytochromobilin) or R²=ethyl (phycocyanobilin). Attachment of these chromophores is always at the 3'-position of the A-ring ethylidene group. The chromophores adopt the Z,Z,Z,s,a configuration in the parental state. The photochemical reaction (photoisomerization of the double bond between rings C and D) is indicated.

causes the addition of a proton to this formerly unprotonated pyrrole ring, thereby yielding a positively charged conjugated pyrrolic system (irrespective of the dissociation of both the propionic side chains that do not contribute to the conjugated system). Protonation of the protein-embedded chromophore has been unambiguously demonstrated by resonance Raman and solid-state ^{15}N NMR spectroscopy.^[4,5]

A wide variation in the spectral properties of bilin photoreceptors has emerged in recent years, as a result of the identification of novel, phytochrome-like proteins, thus extending the well-characterized red–far-red photochromicity into virtually all spectral regions. CBCRs can be considered as “oligo-GAF” domain proteins.^[6] In fact, Cph2 from *Synechocystis* sp. PCC6803 might be considered the first identified phytochrome with a tandem array of GAF domains; some of its photochemical, fluorescence, and physiological properties have recently been reported.^[7] These CBCR GAF proteins are capable of autocatalytically binding the chromophore by employing a single GAF domain.^[8] These properties result in a broad variation of photochemical properties and, because of their relatively small size and their interesting fluorescence properties,^[9] make them valuable tags for intracellular studies.

CBCR GAF domains show an unexpectedly wide variation in absorbance maximum, (virtually the entire spectral range from near UV to the far red). A major subgroup among these CBCR GAF proteins are those generated biosynthetically in a red-absorbing form that can be photoconverted into a green-absorbing photoproduct. The best-characterized GAF domain from this group is that of AnPixJg2 from the cyanobacterium *Anabaena* sp. PCC7120 ($\lambda_{\text{max}} = 648$ nm and 543 nm for Pr and Pg (green-absorbing) forms, respectively),^[8] for which a three-dimensional structure^[10] and micro- to millisecond time-resolved absorption spectroscopy have been determined.^[11] Furthermore, ultrafast measurements (pico- to nanosecond range) have been performed with an AnPixJ orthologue, the GAF4 domain of NpR6012 from *Nostoc punctiforme*; this revealed unexpectedly complex dynamics, probably due to ground- or excited-state heterogeneity.^[12, 13]

Slr1393 from the cyanobacterium *Synechocystis* sp. PCC6803 (another AnPixJ orthologue) is likewise composed of three GAF domains, of which only one (GAF3) is capable of covalently binding a PCB chromophore.^[14] Just as for AnPixJg2, Slr1393-g3 exhibits red/green photochemistry and carries a histidine kinase domain in its C-terminal region for signaling. The high degree of structural similarity was confirmed by a model of SLR1393-g3, when using the structure of AnPixJ as the template (Figure 1). Sequence comparison between the proteins



```

slr1393g3      -LQNIFRATSEDEVRHLLSCDRVLVYRFNPDWSGEFIHESVAQMWE
AnPixJg2      NIDKIFQTTTQEIRQLLCKDRVAVYRFNPDWSGEFVAESVSGSGWV
               ::*:::*:*:*:*****:***. *

slr1393g3      PLKLDQNNFPLWQDYYLQENEGGRYRNHESLAVGDVETAGFTDCH
AnPixJg2      KLVGPDIKT-VWEDTHLQETQGGRYRHQESFVNDIYEAGHFSCH
               * . : : :*:*:*:*:*****:***. *: ** .**

slr1393g3      LDNLRREFIRAFLTVPVFVGEQLWGLLGAYQNGAPRHQWQAREIHL
AnPixJg2      LEILEQEFEIKAYIIVPFAAEKLGWLLAAYQNSGTREWEWESSF
               *: *.***:*.: *****:*.*****.***...* * :

slr1393g3      LHQIANQLGVAVYQAQLLARFQ
AnPixJg2      LTQVGLQFGIAISHAEYLEQTR
               **:..*:*:*:*: *****: :

```

Figure 1. Top, overlay of AnPixJg2 structure (green, PDB ID: 3W2Z) and model structure of SLR1393-g3 (blue). Bottom, sequence alignment of Slr1393-g3 and AnPixJg2. * fully conserved, : semi-conserved, . functionally similar.

revealed high overall similarity, with most of the functionally important amino acids conserved; however, the sequence alignment also identified at strategic positions a number of amino acids that differ between these proteins.

As mentioned above, the micro- to millisecond time-resolved spectroscopy performed on AnPixJ^[11] is the sole study on the conversion of dynamics in CBCR GAF domains. Here we report measurements of the red/green conversion of the orthologue Slr1393-g3 in both directions, in a laser-induced time-resolved experiment aimed at identifying intermediate species in these photochemical processes. In order to determine with greater precision amino acids regulating the red/green conversion process, we performed a more detailed sequence alignment by including other CBCR GAF domains: 24 amino acid differences were identified for Slr1393 in close

proximity to the chromophore compared with the other GAF domains in the alignment.

Results

Design of site-directed mutations, and protein structural and biochemical properties

GAF3 from *Synechocystis* Slr1393 (Slr1393-g3) comprises amino acids L441 to Q596 of the full-length protein. Cysteine 528 has been identified as the sole bilin-binding position.^[14] The structural overlay of Slr1393-g3 and AnPixJG2 (Figure 1) shows virtually complete homology. The selection of amino acids for site-directed mutagenesis was based either solely on sequence alignment (Figure 1, Figure S1 in the Supporting Information; substitutions V463Q, Y464H, N511K, A516K, A516C, E521Y, D527I, and H529Y), or on sequence alignment combined with identification of putative 3D position (L462S, W483M, W496I, T499V, R508N, Y509P, F525A, D527H, D531T, N532Y, R535N, F536M, Y559H, W567E, and E571A). The 3D structure of AnPixJG2 was used, and only amino acids in close proximity to the chromophore were selected for mutation (Figure 2).

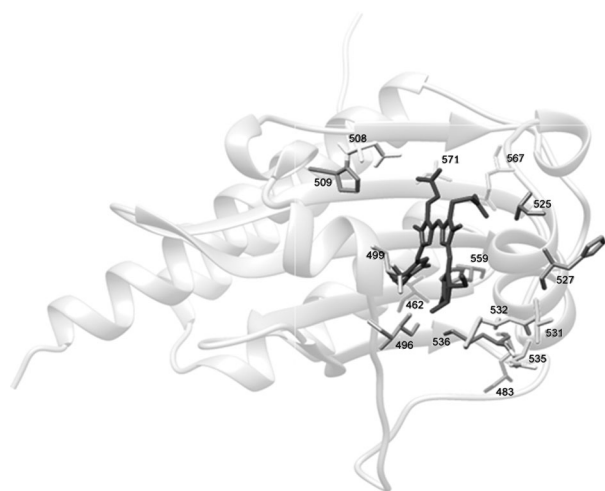


Figure 2. Amino acids of Slr1393-g3 selected for mutagenesis (structure based on that of AnPixJG2).

Wild-type (WT) and mutated Slr1393-g3 proteins were assembled in vivo with PCB by a two-plasmid protocol that makes use of the autocatalytic lyase activity of CBCR GAF domains:^[14] one plasmid encodes the apoprotein and a cotransformed plasmid encodes two enzymes, a heme oxygenase and a phycocyanobilin:ferredoxin oxidoreductase that produces PCB (for details see ref. [14]). All proteins were His-tagged and purified by immobilized metal ion chromatography (IMAC). This procedure, however, purifies both holo- and apoproteins, as assembly of this GAF domain in vivo (i.e., during expression) yields only 30% in the chromophore-loaded form. As an additional purification step, anion exchange chromatography was performed to separate apo- from holoprotein. Routinely, GAF

domains with at least 70% chromophore loading were obtained and used for further studies.

WT-GAF3 of Slr1393 (assembled in vivo) showed an absorbance maximum at 649 nm for the parental state; the photo-product absorbed at 536 nm (Figure 3A and B; the values for AnPixJ are 648 nm and 543 nm, respectively). The mutated proteins could be classified, according to their absorbance properties, into three groups (Table 1): 1) absorbance peaks

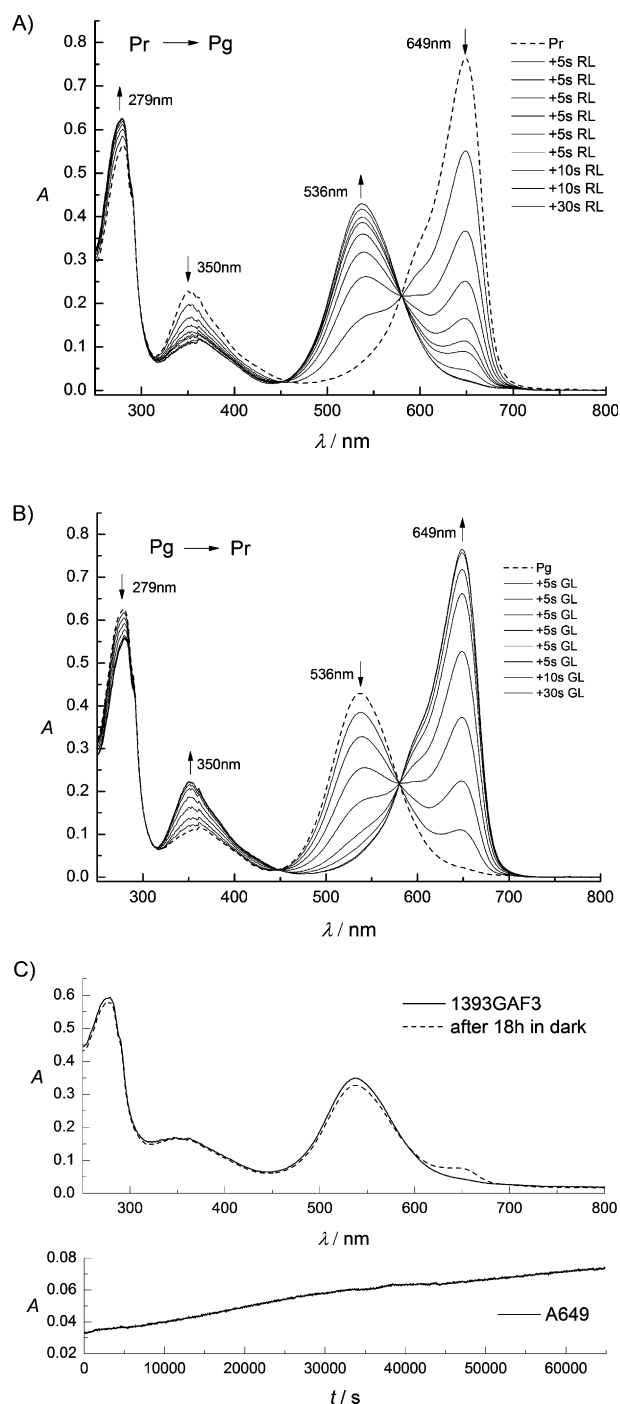


Figure 3. Steady state absorbance spectra of Slr1393-g3 assembled in vivo. A) Red-to-green conversion, B) Green-to-red (back) conversion, C) Stability of the Pg state, recorded over 18 h at 20 °C. LEDs (530 nm, 670 nm) were used for irradiation (duration as indicated).

Table 1. Steady state spectroscopic data of wild-type and mutated Slr1393 GAF3 from *Synechocystis* sp. PCC6803.

	Absorption λ_{max} [nm]		Fluorescence λ_{max} [nm]	
	15E	15Z	15E, (Φ_F)	15Z, (Φ_F)
Proteins obtained from in vivo assembly				
WT	538	648	615 (0.03)	670 (0.06)
L462S	533	649	591 (0.076)	667 (0.031)
W496I	539	623	620 (0.025)	653 (0.063)
R508N	580	649.5	617 (0.021)	667 (0.06)
D531T	553	647	21 (0.029)	668 (0.054)
N532Y	546	651	624 (0.027)	673 (0.045)
	660			
Y559H	553	636	620 (0.014)	658 (0.034)
For both parental and photoproduct states, exchanges at V463Q, Y464H, R465E, W483M, T499V, A516C, A516K, E521Y, D527H, D527I, R535N, F536M, E571A show the same absorbance maxima as wild-type. ^[a]				
Proteins obtained from in vitro assembly				
WT	585	649	645 (0.03)	670 (0.052)
Y509P	580	636	660 (0.012)	662 (0.036)
F525A	580	645	647 (0.028)	668 (0.041)
W567E ^[b]	580	—	636 (0.025)	—

[a] Fluorescence emission maxima for these mutations were around 672 nm for the red-absorbing state (15Z) and around 615 nm for the green-absorbing state (15E). Fluorescence quantum yields for most mutations were less than for the WT protein, except for A516K (0.07 for 15Z form), E521Y (0.064 (15Z)), and R465E (0.065 (15Z)). Extinction coefficients for these mutations were smaller or equal to that of the WT protein except E521Y ($\epsilon = 10 \times 10^4 \text{ M}^{-1} \text{ cm}^{-1}$). [b] This mutation caused loss of photoconvertibility.

comparable to WT, 2) significantly shifted absorbance maxima (either red- or green-absorbing form), and 3) loss of in vivo chromophore binding ability. Some of these unloaded proteins could be furnished with PCB by in vitro assembly (see Table 1).

Steady state spectroscopy and photochemical conversions

The parental, red-absorbing form of Slr1393-g3 ($\lambda_{\text{max}} = 649 \text{ nm}$) could be converted completely into its green-absorbing photoproduct ($\lambda_{\text{max}} = 536 \text{ nm}$) with an isosbestic point at 580 nm. This photoproduct was remarkably thermally stable (Figure 3C): after 18 h, only 6.5% reconverted into the parental (649 nm) form in the dark at 20 °C. Mutants with absorbance maxima nearly identical to that of WT protein were V463Q (650, 539), Y464H (650, 539), R465E (650, 539), W483M (649, 542), T499V (648, 539), A516C (650, 539), A516K (650, 539), E521Y (650, 539), D527H (649, 534), D527I (650, 539), R535N (649, 538), F536M (645, 537), and E571A (648, 535) (absorbance maxima [nm] in brackets for red-, green-absorbing forms, respectively; see also Table 1). Because of the similarity to the WT protein, none of these proteins was subjected to time-resolved measurement, but their fluorescence properties were determined (Table 1).

Similarly, proteins that did not assemble in vivo (or only to a minute amount) were not investigated further in greater detail. This group comprised Y509P, N511K, F525A, H529Y, and W567E; Y509P and F525A showed very small absorbances in the expected spectral range (Table 1) but no photoconversion could be achieved, and W567E showed virtually no absorbance

around 650 nm. Interestingly, three apoproteins of this group could be assembled in vitro. Addition of PCB to Y509P apoprotein yielded a photoconvertible protein with maxima at 636 and 579 nm. The green-absorbing photoproduct, however, showed a broad, unstructured absorbance band. Similar behavior was found for F525A: it also could be assembled in vitro to yield a photoactive protein with an absorbance for the parental form at 645 nm. Also, this mutation led to a photoproduct with an absorbance maximum at 580 nm. Upon in vitro assembly, W567E (the third in this group) yielded only a broad, unstructured absorbance band ($\lambda_{\text{max}} \sim 580 \text{ nm}$), but no photochemical activity could be detected. It should be mentioned in this context that photoproducts with broad unstructured absorbance bands around 580 nm (R508N upon in vivo assembly, Y509P and W567E in vitro) were also obtained for the WT protein, if expressed as apoprotein and furnished in vitro with PCB. For a protein obtained as such, the WT apoprotein yields a parental form with an absorbance maximum (650 nm) identical to that of the in vivo assembled protein, however, irradiation yields a 585 nm form (Figure 4), which could be converted into the 650 nm red-absorbing form.

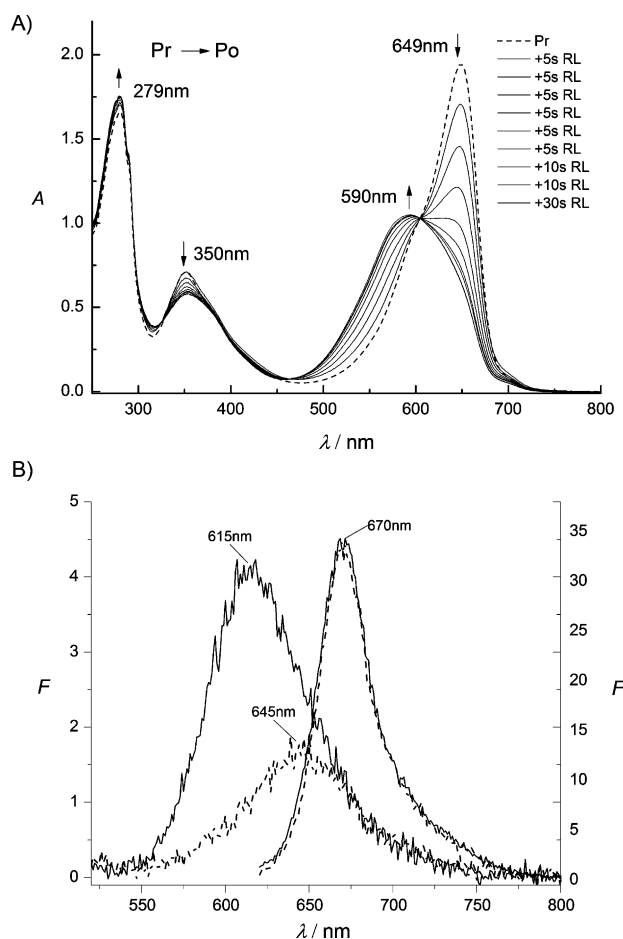


Figure 4. Photoconversion and fluorescence properties of Slr1393-g3 assembled in vitro. A) Steady-state absorbance changes for conversion of the red- to the orange-absorbing form of the photoproduct (Po). B) Fluorescence emission spectra for the in vitro assembled GAF3 domain of Slr1393, for parental and photoproduct state (----); the corresponding spectra of the in vivo assembled (WT) protein are shown for comparison (—).

The most interesting mutations were those that caused a spectral shift for the parental or photoproduct state (or for both). This group comprised mutations L462S (649, 533 nm, red-, green-absorbing forms, respectively), W496I (623, 539), R508N (649, 600; photoproduct absorbance band very broad and unstructured), D531T (647, 553), and Y559H (636, 553). The most interesting mutation in this group was N532Y: upon red light irradiation (LED at 670 nm) a parental peak at 651 nm converted into a species with 546 nm absorbance maximum, but concomitantly formed an even further red shifted absorbance band (peak 660 nm; Figure 5). LED irradiation (530 nm) of the short wavelength part of this photoproduct fully reformed the parental red-absorbing state. In contrast, irradiation of the long wavelength absorbance of the photoproduct ($\lambda_{\text{ex}} = 700$ nm) led to very little change to the parental state.

Some of the mutated proteins from this group were minimally loaded with chromophore (L462S, 1.5% relative to WT; W496I, 5%; Y559H, 1%). These proteins were not studied further, other than for their fluorescence properties.

Fluorescence spectroscopy

The fluorescence of WT-Slr1393-g3 was reported recently.^[9,14] This protein fluoresces in both states (red and green; Figure 4), yet with different quantum yields ($\lambda_{\text{em}} = 670$ and 615 nm, $\Phi_{\text{fl}} = 0.06$ and 0.03, respectively). For all mutations, the fluorescence yields were equal to or smaller than for the WT protein. Some small shifts (a few nanometers) in the emission maxima were detected. The largest changes in fluorescence emission were for proteins that showed a shifted absorbance maximum for the photoproduct around 580 nm (instead of 539 nm): in vitro assembled WT protein ($\lambda_{\text{max}} = 590$ nm, $\lambda_{\text{em}} = 645$ nm; Figure 4; cf. in vivo assembled WT: $\lambda_{\text{max}} = 538$ nm, $\lambda_{\text{em}} = 615$ nm), F525A ($\lambda_{\text{max}} = 580$ nm, $\lambda_{\text{em}} = 647$ nm), and W567E ($\lambda_{\text{max}} \sim 570$ nm, $\lambda_{\text{em}} = 636$ nm).

Laser-induced, time-resolved absorbance changes for WT Slr1393-g3

Currently, there is only one report of time-resolved absorbance changes in the micro- to millisecond time range performed with AnPixJg2.^[11] As Slr1393-g3 is orthologous yet shows (for both red- and green-absorbing states) outstanding thermal stability in the dark (see above), it should be well suited for laser flash photolysis. Excitation of the red-absorbing form initiated three conversion processes, indicative of the transient formation of two intermediates. Global fit analysis of these absorbance changes yielded lifetimes of 3.2 μs , 390 μs , and 1.5 ms (Figure 6). In lifetime-associated difference spectra (LADS) negative amplitudes indicate the formation of intermediates, and positive amplitudes reflect their decay. The 3.2 μs component shows the formation of an intermediate with a (difference) absorbance maximum at around 630–640 nm. This intermediate decays (390 μs) into an intermediate with an absorbance maximum at around 590 nm (close to the isosbestic point). This conversion shows very shallow absorbance differences, apparently a result of partial overlap of the

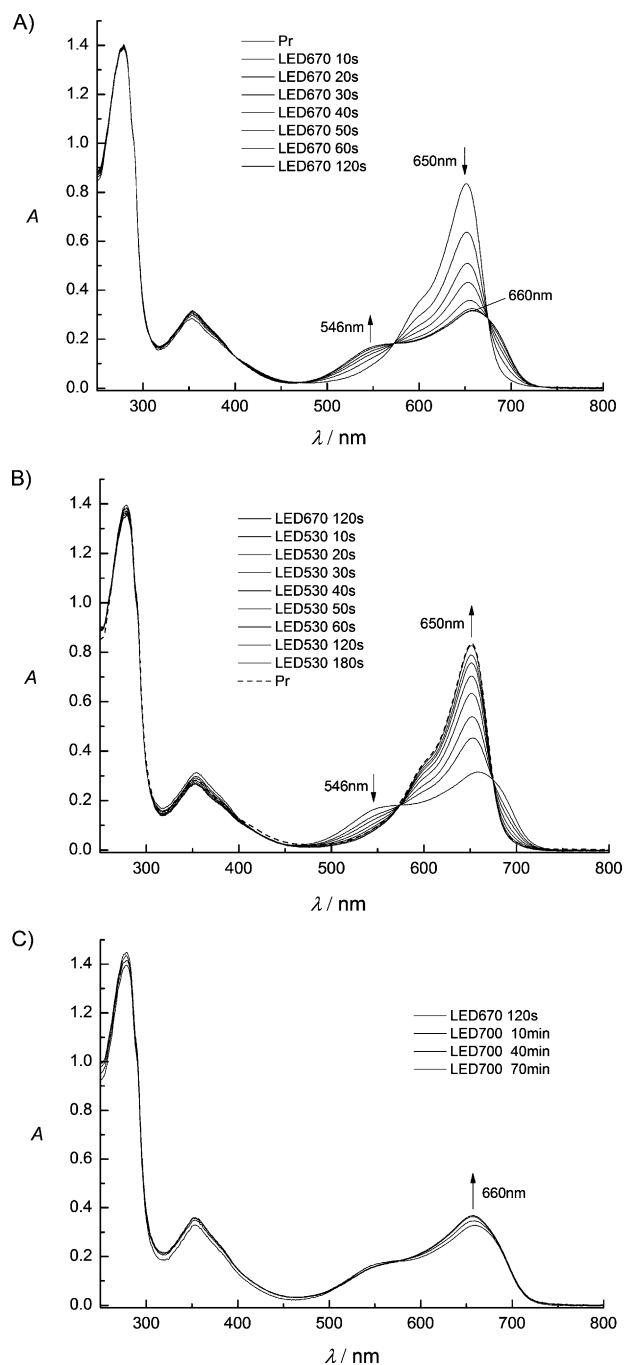


Figure 5. Steady-state photoconversion of N532Y mutant of Slr1393-g3. A) Conversion of the red-absorbing parental state into the photoproduct (spectrum with the highest absorbance at 660 nm is the dark-adapted parental state). Irradiation wavelength is 670 nm. Conversion is shown after 10, 20, 30, 40, 50, 60, and 120 s of irradiation. Arrows indicate the absorbance changes. B) Reconversion of the photoproduct into the parental state by irradiation with 530 nm light. Spectrum with lowest absorbance at 650 nm corresponds to 120 s irradiation curve in the upper panel. Spectra are shown after irradiation for 10, 20, 30, 40, 50, 60, 120, and 180 s. Dotted curve (spectrum with highest absorbance at 650 nm) shows the dark-adapted parental state before irradiation ($t = 0$). C) Re-conversion of the photoproduct into the parental state by irradiation at 700 nm. Spectrum with lowest absorbance at 650 nm corresponds to parental state irradiation for 120 s (final trace in the upper most panel). Note that here irradiation was performed over 70 min (10 + 30 + 30).

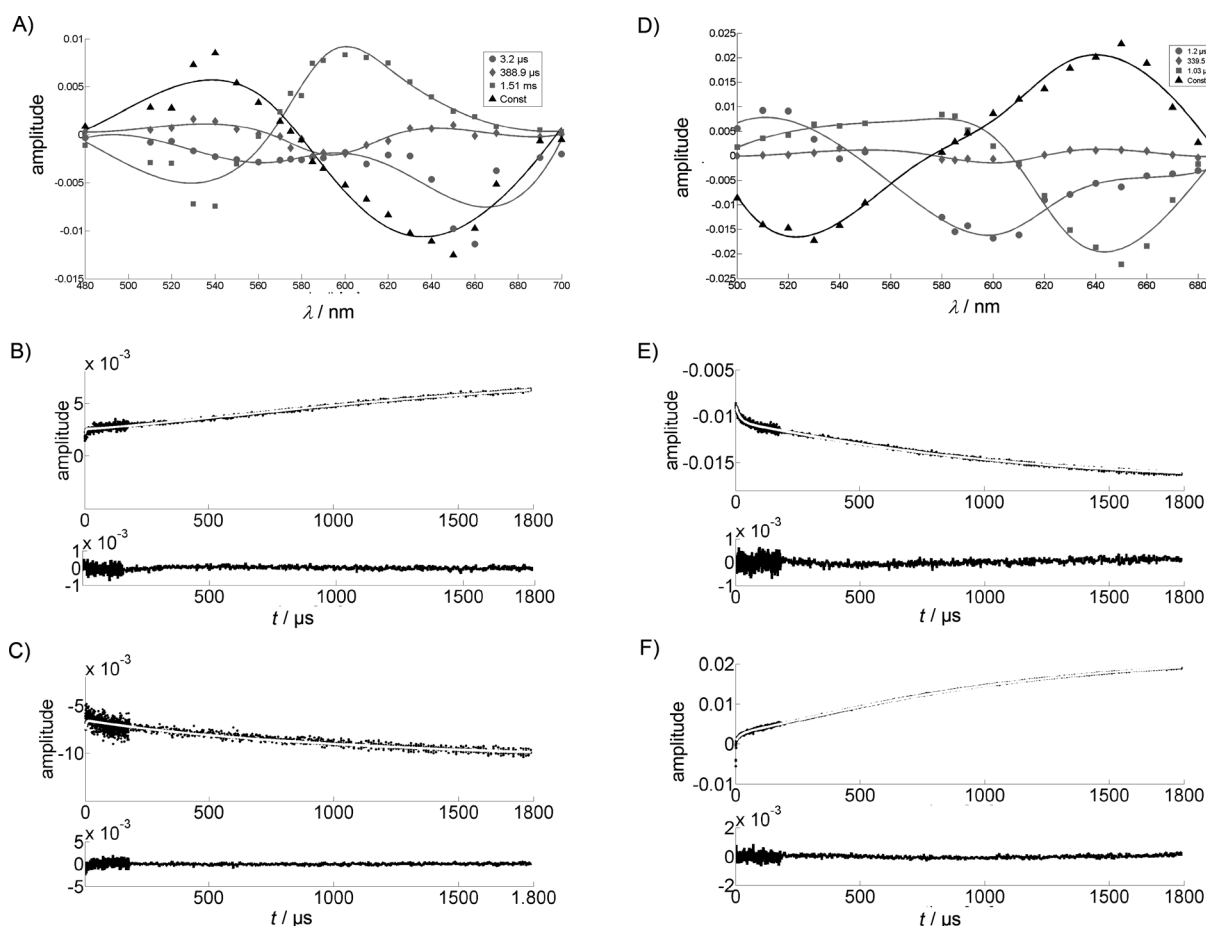


Figure 6. LADS of Slr1393. A) Conversion of the parental state into the green-absorbing photoproduct. $\lambda_{\text{ex}} = 650$ nm. Fit and residuals are shown for B) 540 and C) 640 nm, respectively. D) Conversion of the photoproduct into the parental state by 540 nm irradiation. Fit and residuals are shown for E) 530 and F) 650 nm, respectively.

intermediates' difference spectra and a low transient concentration of this intermediate. The final conversion (lifetime 1.5 ms) with an intense positive amplitude around 600 nm and a negative lobe around 530 nm indicates decay of the 590 nm intermediate and formation of the final green-absorbing photoproduct ($\lambda_{\text{max}} = 530$ nm).

The photochemistry of the green-absorbing form (excitation at 540 nm) also displayed three lifetimes (1.2 μs , 340 μs , and 1.03 ms), corresponding to the formation and decay of two intermediates. The 1.2 μs process shows the decay of the starting state (positive amplitude of LADS) and the formation of an intermediate with $\lambda_{\text{max}} = 600$ nm. This lifetime of 340 μs shows very little absorbance change and might be simply a consequence of conformational rearrangement with only small effects on the absorbance properties of this intermediate. The major process (formation of the 650 nm red-absorbing form) takes place 1.03 ms.

The finding that both conversion processes are dominated by only one intermediate (on this timescale) is yet more evident from the simple difference spectra taken at selected time points (Figure 7). Interestingly, both conversions show isosbestic points at 565 nm for the red-to-green conversion and approximately 605 nm for the green-to-red conversion, thus indi-

cating that formation of these intermediates is much faster than the conversion into the final product, thereby keeping formation and decay of the intermediates well separated and yielding the isosbestic points.

Time-resolved absorbance spectroscopy of the in vitro assembled wild-type proteins and of selected mutants

Conversion kinetics for the in vitro assembled protein and for mutations that showed absorbance properties that differed from those of the WT were followed at selected wavelengths. These experiments were performed at wavelengths at which maximum absorbance changes were expected, for example, the wavelength of maximum bleaching of the parental state or of maximum formation of the photoproduct. At these wavelengths, the absorbance changes were compared to those at the corresponding wavelengths of the WT protein assembled in vivo (Figure 8, Table 2).

The WT protein assembled in vitro showed an absorbance at 648 nm, which is identical to that for the protein assembled in vivo. The photoproduct, however, was less hypsochromically shifted (absorbance ~ 590 nm). Formation of the photoproduct (excitation at 650 nm) was followed at 500, 520, 540, and

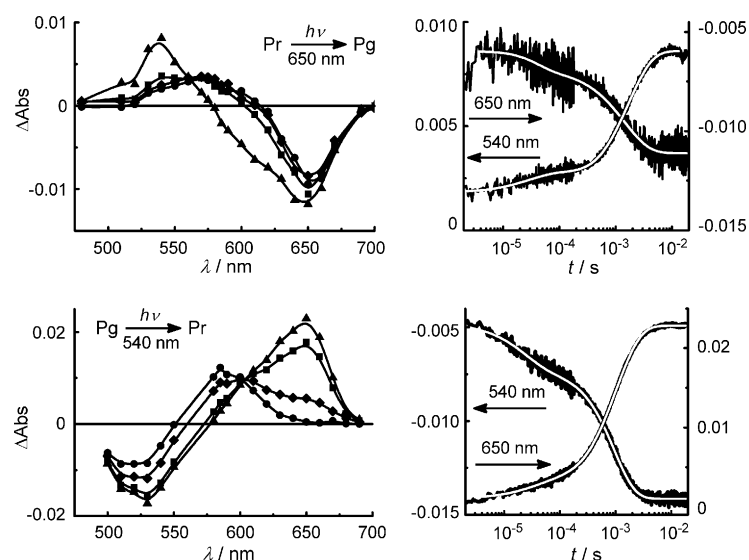


Figure 7. Left: difference spectra for conversion of the in vivo assembled WT protein; top: conversion of red- into green-absorbing form; time points for difference spectra and excitation wavelength are: \bullet : 5 μs , \blacklozenge : 50 μs , \blacksquare : 500 μs , \blacktriangle : 4 ms. Bottom: green-to-red conversion; time points are: \bullet : 2 μs , \blacklozenge : 230 μs , \blacksquare : 1.5 ms, \blacktriangle : 18 ms. Right: wavelengths most indicative for the conversions selected; top: red-to-green conversion, bottom: green-to-red conversion. Arrows identify the y-axis for the respective wavelength.

560 nm. Two dominant lifetimes ($\sim 30 \mu\text{s}$ and $\sim 2 \text{ ms}$) were obtained from these single-wavelength fits; the corresponding lifetimes for the WT protein assembled in vivo (fitted for the same wavelengths kinetics) were 300 μs and 1.5 ms. Back-conversion of the photoproduct into the parental red-absorbing state (excitation at 540 nm, detection at 650 nm) for the in vitro assembled protein occurred with two lifetimes ($\sim 13 \mu\text{s}$ and 1.3–1.5 ms); the corresponding values for the WT protein with these excitation and detection wavelengths were approximately 0.9 μs and 1.1 ms.

The red-to-green conversion of mutant D531T (absorbance maxima of 648 and 554 nm for Pr and Pg, respectively) took place with a single lifetime ($\sim 1.1 \text{ ms}$); re-formation of the parental red-absorbing state occurred with two lifetimes ($\sim 1.7 \mu\text{s}$ and 1 ms). Mutation R508N showed a red-absorbing parental state at $\lambda_{\text{max}} = 650 \text{ nm}$, but irradiation generated a very broad, unstructured absorbance peak ($\lambda_{\text{max}} = 590\text{--}600 \text{ nm}$) with significant overlapping with the region of the parental state. Formation of the photoproduct ($\sim 330 \mu\text{s}$) was faster than for the WT protein.

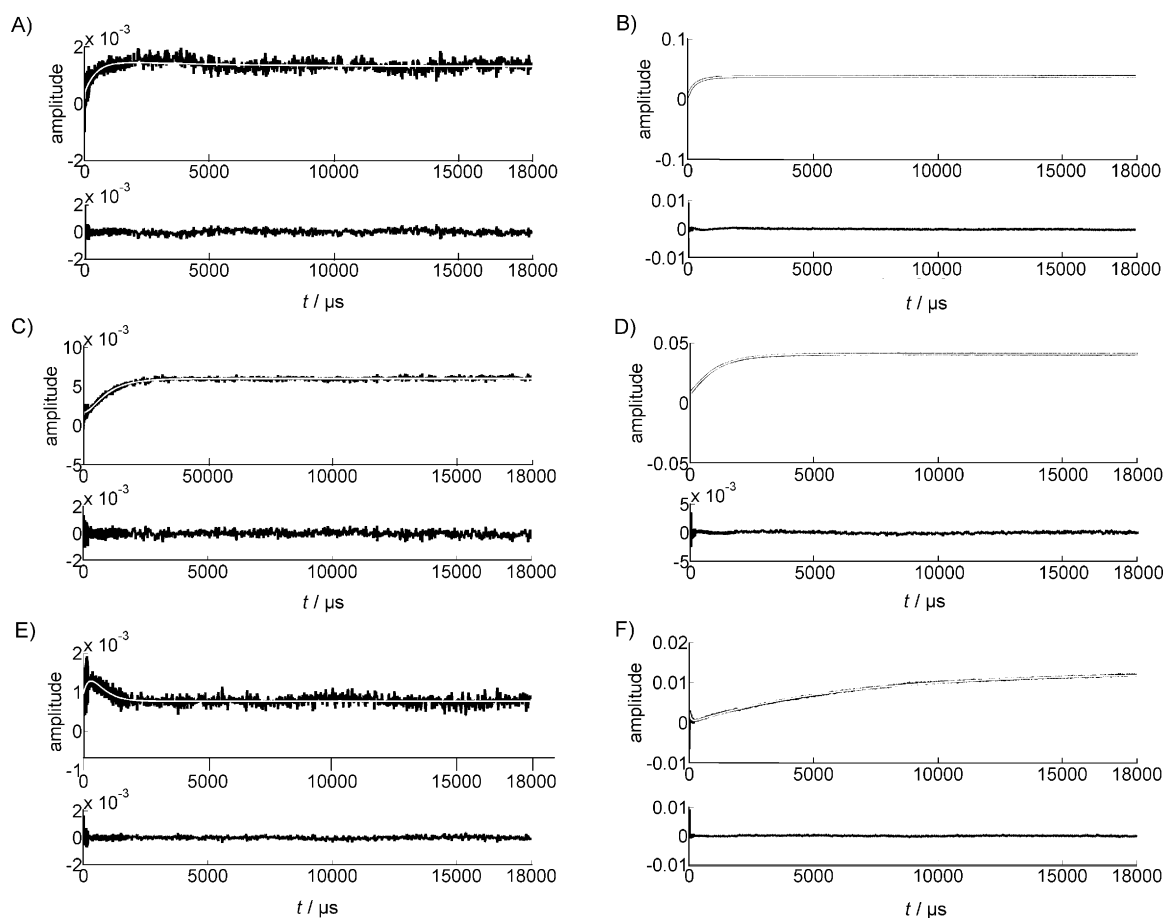


Figure 8. Selected kinetics for mutations R508N, D531T, and N532Y; single-wavelength recordings are shown together with (below) residuals after fitting with the lifetimes in Table 2. Figure shows conversion of parental into photoproduct state, and photoproduct into parental state conversions (below). Excitation/detection wavelengths [nm]: R508N, 670/540, 530/650; D531T, 650/520, 540/650; N532Y, 650/540, 525/650.

Table 2. Intermediate lifetimes from laser flash photolysis for wild-type in vivo assembled Slr1393 and selected mutations (red-to-green and green-to-red conversion).

	τ_1 [μ s]	τ_2 [μ s]	τ_3 [ms]
WT (in vivo assembly)			
parental-to-photoproduct ^[a]	3.2	390	1.5
photoproduct-to-parental ^[a]	1.2	340	1.03
WT (in vitro assembly)			
650/520 ^[b]	20 (26)	– (300)	2.4 (1.5)
540/650 ^[b]	1 (1.3)	24 (360)	1.5 (1)
R508N			
670/540 ^[b]	7.4 (26)	470 (300)	4.55 (1.5)
530/650 ^[b]	– (1.3)	113 (360)	0.45 (1)
D531T			
650/520 ^[b]	14 (26)	260 (300)	0.8 (1.5)
540/650 ^[b]	1.9 (1.3)	355 (360)	0.94 (1)
N532Y			
650/540 ^[b]	7.5 (26)	390 (300)	– (1.5)
650/710 ^[b,c]	2.5 (–)	470 (–)	– (–)
525/650 ^[b]	73 (1.3)	– (360)	6.2 (1)

[a] From global fit. [b] Wavelength for excitation/detection; for each mutation forward and (following line) backward reactions are given. Values in brackets refer to the lifetimes of the in vivo assembled WT protein, measured at the same wavelength, determined from single wavelength fit. [c] The in vivo assembled WT protein did not show detectable absorbance changes.

Re-formation of the parental state from the photoproduct ($\sim 310 \mu$ s) was also found to be faster than for the WT protein. Mutant N532Y formed the green-absorbing photoproduct with shorter kinetics than those observed for the WT protein. Biexponential fit yielded lifetimes of 1.5–2 μ s and approximately 400 μ s. As this mutation gave rise also to a long-wavelength absorbance of the photoproduct, absorbance changes were also detected at 710 nm; at this wavelength, lifetimes similar to that of the green-absorbing lobe were again detected, thus indicating that this absorbance is, in fact, part of the photoproduct. The re-conversion into the parent state was also fitted biexponentially: approximately 1 μ s and approximately 60 μ s. For this mutant, both the forward and reverse conversions were faster than for the WT protein.

Discussion

GAF domains from CBCR photoreceptors have expanded the range of photochemical processes of bilin-binding chromoproteins to an unexpected extent. Not only do these proteins accomplish photochromic photoisomerization reactions with just isolated GAF domains, they also perform chemical reactions not found for canonical phytochromes, by isomerizing the covalently bound phycocyanobilin into phycoviolobilin or bilirubin-type chromophores.^[19–22] Red/green switching proteins comprise a large subclass of identified proteins with GAF domains.^[6] Despite their potential as tools in microscopy,^[9] relatively few functional studies have been performed with CBCR GAF domains. The GAF3 domain from Slr1393 (*Synechocystis* sp. PCC6803) shows 49% sequence identity to AnPixJ and shares most of the significant amino acids. Unlike AnPixJ, which slowly reverts thermally from the photoproduct to the

parental state,^[8] Slr1393-g3 is essentially thermally stable in its green-absorbing photoproduct state. Thus, its great photochromic shift (~ 110 nm) allows full conversion from the parental into the photoproduct state and is optimal for time-resolved spectroscopy (usually several laser flash experiments have to be accumulated in order to improve signal-to-noise ratio).

The lifetimes for both red-to-green and green-to-red conversions indicate a relatively simple photochemistry of CBCR GAF domains, with only two intermediates in each direction. One has to keep in mind, however, that ultrafast measurements in the picosecond range performed with NpR6012 have identified very short-lived, red-shifted intermediates as direct products of the photoisomerization process. The relatively simple conversions observed in isolated GAF domains from CBCRs differ from the photochemistry of canonical phytochromes, which show more complex formation of Pr and Pfr states.^[23,24] Yet, in the photochemistry of both canonical phytochromes and these phytochrome-like proteins the initial step is formation of a red-shifted intermediate, thus reflecting the increase in distance between the protonated, positively charged chromophore and its counterion.^[13,25,26] Such a bathochromic primary intermediate (indicating an increase in positive charge on the double-bond system of the chromophore) is common across protonated photoactive chromophores and has long been observed (e.g., in retinal proteins).^[27,28]

The overall simpler photoconversion process in these isolated CBCR GAF domains (relative to canonical phytochromes) might be attributable to the much smaller protein size, which allows following more readily the constraints of chromophore isomerisation. However, one has to keep in mind that so far only isolated GAF domains have been studied; full-length proteins might exhibit more complex, but definitely longer-lasting, conversion reactions.

Proteins carrying mutations that cause shifts in absorbance maxima (from those of the WT protein) of only few nanometers showed similar conversions between both states, in terms of absorbance maxima of the intermediates as well as computed lifetimes. The in vitro assembled protein, however, exhibited a less hypsochromically shifted photoproduct state ($\lambda_{\text{max}} = 590$ nm) and slightly slower conversion kinetics than for the WT protein; this probably indicates somewhat different folding of the polypeptide chain. Interestingly, the parental state was not influenced by the assembly (in vivo or in vitro). Specifically, one might assume that the photoisomerization of the PCB chromophore generates a “more-or-less” positively charged chromophore, affected by small conformational differences depending on amino acids in the surrounding pocket, as has similarly been recently proposed for AnPixJ.^[29] Mutant R508N showed a very broad, unstructured absorbance band for the photoproduct state, and apparently followed a clearly different photochemical pathway, as both reactions (forward and backward) were faster than for the WT protein.

Overall, the kinetic and steady-state data for the isolated CBCR GAF3 domain of Slr1393 presented here identify these proteins as novel and notably different to canonical phytochromes. In addition, the different behaviors observed for in

vivo and in vitro assembly were unexpected and indicate very subtle interactions between the chromophore and the protein, as well as between different regions of the polypeptide chain. Thus, the presence of the chromophore during polypeptide synthesis is essential for three-dimensional folding to guarantee a properly functioning protein. The mutations at several positions close to the chromophore demonstrate the important role of the amino acids in the binding pocket for the absorbance and kinetic properties of these proteins.

Experimental Section

Genes and proteins: Cloning of *slr1393 gaf3* has been described formerly.^[14] Mutations V463Q, Y464H, N511K, A516K, A516C, E521Y, D527I, and H529Y were introduced by using a MutanBEST mutation kit (TaKaRa, Otsu, Japan). Mutated genes encoding exchanges L462S, W483M, W496I, T499V, R508N, Y509P, F525A, D527H, D531T, N532Y, R535N, F536M, Y559H, W567E, and E571A were purchased from Genscript (<http://www.genscript.com/>). The positions for mutagenesis were identified from an alignment (ClustalW) with sequences of AnPixJ and TePixJ (see the Supporting Information). The three-dimensional model of Slr1393-g3 was constructed from AnPixJ as the template (PDB ID: 3W2Z) by using Modeller (version 9.11, <http://salilab.org/modeller/>).

For in vivo chromophore assembly, WT and mutated Slr1393-g3 proteins were expressed by following a two-plasmid transformation/expression protocol.^[14] All recombinant proteins carried an N-terminal His-tag for IMAC. After elution from the Ni-affinity column, imidazole was removed by dialysis against Tris buffer (50 mM, pH 7.2) containing NaCl (50 mM) and EDTA (5 mM). Protein was then loaded onto a HiPrep DEAE FF 16/10 ion-exchange column (GE Healthcare) to remove most of the unloaded apoprotein, by making use of different isoelectric points for apo- and holoprotein. The proteins were eluted in a linear gradient of NaCl (50 mM to 1 M) in dialysis Tris buffer. Purified protein was concentrated for further studies, and the purity was confirmed by PAGE (4–12% Bis-Tris Novex NuPAGE Gel, Life Technologies).

Steady-state spectroscopy: Steady-state absorbance and fluorescence spectra were recorded at 20 °C with a UV-2401 spectrophotometer (Shimadzu) and a Cary Eclipse Fluorescence Spectrophotometer (Varian); for determination of fluorescence yields, values of 0.03 (Pg), 0.06 (Pr), reported for the WT protein were used as reference.^[9] The stability at 20 °C of each state (red- or green-absorbing) was followed over time by a kinetics-recording program supplied with the spectrophotometer at selected wavelengths. Photoconversion between the red- and the green-absorbing states was performed by exhaustive irradiation from LEDs of the appropriate wavelengths (530 nm, 670 nm; Roithner LaserTechnik, Vienna, Austria).

Laser-induced time-resolved absorbance spectroscopy: The third harmonic of a Nd:YAG laser (InnoLas) was used to drive an OPO (GWU, built into the InnoLas cage), thus allowing excitation from approximately 410 nm to the near infrared. The intensity of the laser pulse (~10 ns) ensured a linear range of absorbance changes to avoid photochemical artifacts (≤ 10 mJ per pulse). Transient absorbance changes were measured by a home-built detection system. Excitation and detection light were perpendicular (i.e., a crossed-beam arrangement). The sample was placed between two matched monochromators: slave, f/3.4 (Applied Photophysics, Leatherhead, UK); master, f/4.2 (Photon Technology, Edison, NJ). A continuous wave (cw) 75 W Xenon lamp (Amko) was used. Absorb-

ance changes ($(20 \pm 1)^\circ\text{C}$) were detected with a R3896 photomultiplier (Hamamatsu, Hamamatsu City, Japan); data were recorded on a TDS 744A oscilloscope (Tektronix). After each laser pulse, the samples were returned to their initial absorbance by cw irradiation from a halogen projector lamp with appropriate filters, or from an LED of matched wavelength (530 nm, 90–120 mW; 670 nm, 60 mW). Independent control experiments demonstrated that the back-irradiation time (530 nm, 5 s; 670 nm, 8 s) was sufficient to revert any photoproduct generated by the laser flash. LEDs were approximately 4 cm from the sample cuvette.

The concentrations of samples of Slr1393-g3 were adjusted to $A = 0.3$ – 0.5 at their absorbance maxima; control absorbance spectra (taken before and after one set of experiments) showed no absorbance change, which would be indicative of protein denaturation or photochemical side reactions. Samples were excited at 650 nm (red-to-green state conversion) or at 540 nm (reverse process). Absorbance changes were monitored for 17 wavelengths in 10 nm steps (510–670 nm). Around the isosbestic point (580 nm), absorbance changes were also followed at 575 nm and 585 nm; in addition, absorbance at 480 nm, 690 nm, and 700 nm was detected to identify changes far from the steady-state maxima. The kinetics were recorded in three time windows to allow sufficient signal quality, and at short time intervals (0–200 μs , 0–2 ms, 0–20 ms, full scale). At least five single laser pulses were averaged for each individual detection wavelength to improve signal-to-noise ratio.

Data handling and fit procedures: Kinetics traces (above) were normalized for maximum amplitude and then merged into a single time window to cover the entire time range (0.5 μs to 20 ms). The merged traces were then subjected to global fit analysis.^[15] The identified processes for each lifetime were plotted as LADS (for details, see refs. [16]–[18]). By convention, a graphical presentation of LADS uses negative amplitude for formation of a particular intermediate, and positive amplitude for disappearance of the intermediate.

Acknowledgements

We greatly acknowledge the expert technical help of Leslie Currell, Norbert Dickmann, and Dirk Kampen during the laser flash photolysis experiments, and of Gülümse Koc (all MPI-CEC) during the fluorescence spectroscopy measurements. Also, we are grateful to Silvia E. Braslavsky, MPI-CEC, and to Igor Chizhov, University of Hannover, for their valuable contributions during discussion of the results. L.V. wishes to thank the German Academic Exchange Service, DAAD, for a travel grant. C.B. thanks the Argentinian funding agencies CONICET (PIP-0374/12) and FONCYT (PICT-2666/12). K.H.Z. is grateful for support (grants 31110103912 and 31270893) by the National Natural Science Foundation of China. X.X. is recipient of a grant from the scientific arrangement between CAS (Chinese Academy of Sciences) and the Max Planck Society. K.T. is a recipient of a grant from CSC (China Scholar Council).

Keywords: chromophores • global fit • mutagenesis • phycocyanobilin • phytochromes • time resolved

[1] B. L. Montgomery, J. C. Lagarias, *Trends Plant Sci.* **2002**, 7, 357–366.

[2] N. C. Rockwell, J. C. Lagarias, *ChemPhysChem* **2010**, 11, 1172–1180.

- [3] C. Hill, W. Gärtner, P. Towner, S. E. Braslavsky, K. Schaffner, *Eur. J. Biochem.* **1994**, *223*, 69–77.
- [4] M. A. Mroginiski, D. von Stetten, F. V. Escobar, H. M. Strauss, S. Kaminski, P. Scheerer, M. Günther, D. H. Murgida, P. Schmieder, C. Bongards, W. Gärtner, J. Mailliet, J. Hughes, L.-O. Essen, P. Hildebrandt, *Biophys. J.* **2009**, *96*, 4153–4163.
- [5] T. Rohmer, H. Strauss, J. Hughes, H. de Groot, W. Gärtner, P. Schmieder, J. Matysik, *J. Phys. Chem. B* **2006**, *110*, 20580–20585.
- [6] M. Ikeuchi, T. Ishizuka, *Photochem. Photobiol. Sci.* **2008**, *7*, 1159–1167.
- [7] K. Anders, D. von Stetten, J. Mailliet, S. Kiontke, V. A. Sineshchekov, P. Hildebrandt, J. Hughes, L.-O. Essen, *Photochem. Photobiol.* **2011**, *87*, 160–173.
- [8] R. Narikawa, Y. Fukushima, T. Ishizuka, S. Itoh, M. Ikeuchi, *J. Mol. Biol.* **2008**, *380*, 844–855.
- [9] J. Zhang, X.-J. Wu, Z.-B. Wang, Y. Chen, X. Wang, M. Zhou, H. Scheer, K.-H. Zhao, *Angew. Chem. Int. Ed.* **2010**, *49*, 5456–5458; *Angew. Chem.* **2010**, *122*, 5587–5590.
- [10] R. Narikawa, T. Ishizuka, N. Muraki, T. Shiba, G. Kurisu, M. Ikeuchi, *Proc. Natl. Acad. Sci. USA* **2013**, *110*, 918–923.
- [11] Y. Fukushima, M. Iwaki, R. Narikawa, M. Ikeuchi, Y. Tomita, S. Itoh, *Biochemistry* **2011**, *50*, 6328–6339.
- [12] P. W. Kim, L. H. Freer, N. C. Rockwell, S. S. Martin, J. C. Lagarias, D. S. Larsen, *Biochemistry* **2012**, *51*, 619–630.
- [13] P. W. Kim, L. H. Freer, N. C. Rockwell, S. S. Martin, J. C. Lagarias, D. S. Larsen, *Biochemistry* **2012**, *51*, 608–618.
- [14] Y. Chen, J. Zhang, J. Luo, J.-M. Tu, X.-L. Zeng, J. Xie, M. Zhou, J.-Q. Zhao, H. Scheer, K.-H. Zhao, *FEBS J.* **2012**, *279*, 40–54.
- [15] S. E. Braslavsky, W. Gärtner, K. Schaffner, *Plant Cell Environ.* **1997**, *20*, 700–706.
- [16] I. V. Chizhov, D. S. Chernavskii, M. Engelhard, K.-H. Mueller, B. V. Zubov, B. Hess, *Biophys. J.* **1996**, *71*, 2329–2345.
- [17] K.-H. Müller, T. Plessner, *Eur. Biophys. J.* **1991**, *19*, 231–240.
- [18] K.-H. Müller, H. J. Butt, E. Bamberg, K. Fendler, B. Hess, F. Siebert, M. Engelhard, *Eur. Biophys. J.* **1991**, *19*, 241–251.
- [19] N. C. Rockwell, S. L. Njuguna, L. Roberts, E. Castillo, V. L. Parson, S. Dwojak, J. C. Lagarias, S. C. Spiller, *Biochemistry* **2008**, *47*, 7304–7316.
- [20] N. C. Rockwell, S. S. Martin, K. Feoktistova, J. C. Lagarias, *Proc. Natl. Acad. Sci. USA* **2011**, *108*, 11854–11859.
- [21] T. Ishizuka, R. Narikawa, T. Kohchi, M. Katayama, M. Ikeuchi, *Plant Cell Physiol.* **2007**, *48*, 1385–1390.
- [22] T. Ishizuka, A. Kamiya, H. Suzuki, R. Narikawa, T. Noguchi, T. Kohchi, K. Inomata, M. Ikeuchi, *Biochemistry* **2011**, *50*, 953–961.
- [23] P. Schmidt, U. H. Westphal, K. Worm, S. E. Braslavsky, W. Gärtner, K. Schaffner, *J. Photochem. Photobiol. B* **1996**, *34*, 73–77.
- [24] I. V. Chizhov, B. Zorn, D. J. Manstein, W. Gärtner, *Biophys. J.* **2013**, *105*, 2210–2220.
- [25] M. G. Müller, I. Lindner, I. Martin, W. Gärtner, A. R. Holzwarth, *Biophys. J.* **2008**, *94*, 4370–4382.
- [26] J. Dasgupta, R. R. Frontiera, K. C. Taylor, J. C. Lagarias, R. A. Mathies, *Proc. Natl. Acad. Sci. USA* **2009**, *106*, 1784–1789.
- [27] R. A. Mathies in *Frontiers in Biochemical and Biophysical Studies of Proteins and Membranes* (Ed.: Teh-Yung Liu), Elsevier, **1983**, pp. 367–386.
- [28] P. Tavan, K. Schulten, D. Oesterhelt, *Biophys. J.* **1985**, *47*, 415–430.
- [29] F. Velasquez Escobar, T. Utesch, R. Narikawa, M. Ikeuchi, M. A. Mroginiski, W. Gärtner, P. Hildebrandt, *Biochemistry* **2013**, *52*, 4871–4880.

Received: January 23, 2014

Published online on April 24, 2014